Approaches for Improving Lumped Parameter Thermal Networks for Outer Rotor SPM Machines

Approaches for Improving Lumped Parameter Thermal Networks for Outer Rotor SPM Machines

Daniel Wöckinger*, Gerd Bramerdorfer*, *Senior Member, IEEE*,
Silvio Vaschetto§, *Senior Member, IEEE*, Andrea Cavagnino§, *Fellow, IEEE*,
Alberto Tenconi§, *Senior Member, IEEE*, Wolfgang Amrhein*, and Frank Jeske†

* Department of Electrical Drives and Power Electronics, Johannes Kepler University Linz, Linz, Austria
§ Dipartimento Energia, Politecnico di Torino, Turin, Italy
† Ebm-papst St. Georgen GmbH & Co. KG, St. Georgen, Germany
Email: daniel.woeckinger@jku.at

***Abstract*—This work is about the transient modeling of the thermal characteristics of outer rotor SPM machines by considering a lumped parameter thermal network based approach. The machine considered here poses particular challenges for the modeling, e.g., due to the semi-closed stator surrounded by a rotor bell that provides a speed-dependent cooling of the stator coils. Starting from a simpler basic network configuration, model extensions and refinements are presented and discussed. The subsequent parameter identification is done by means of an initial design of experiments based sampling, and a subsequent single-objective and also a multi-objective optimization of error functions for the components' temperatures. Analyzing the therefrom derived Pareto fronts and the consequent tradeoff regarding achievable minimum modeling errors for different system's components gives insights into where and how the modeling can be further improved. All the investigations are based on experimental results obtained through operating a particularly developed test setup.**

***Index Terms*—electric machines, evolutionary algorithm, lumped parameter thermal network, optimization, outer rotor, permanent magnet synchronous machines**

I. Introduction

An accurate temperature prediction for major components of electric machines is crucial. A precise determination of the thermal circumstances facilitates driving such devices at maximum possible load and thus gaining highest utilization. Furthermore, an in-depth understanding of the overall thermal behavior at various operating points and different installation situations can avoid over-engineering. By setting proper boundaries, safety and reliability related aspects can be properly considered. While often the focus was on predicting machine temperatures for static conditions, nowadays it is of highest interest to correctly estimate thermal aspects and thus possible operational limits for the transient case. For this reason, some previous analyses were at least partially based on simulations, e.g., CFD-based modeling [1], [2]. Additionally, a significant number of modeling approaches focuses on characterizing thermal models based on experimental results [3], [4]. In both cases, it is tried to minimize the overall effort for obtaining an accurate modeling. Besides the classical modeling approaches, these days researchers deal with emerging technologies, e.g., machine learning (ML-) based approaches [5]. This gives maximum flexibility for achieving high modeling accuracy, as well as regarding which inputs and outputs are selected for modeling. While in approaches based on the underlying physics, usually the losses are set as inputs, the more flexible ML-based approaches allow for alternatively specifying, e.g., torque and speed of the machine as inputs. The latter, however, necessitates an experimental setup or any other further source for acquiring the data used for the modeling. A major drawback of such modern approaches is that the heat flows in the electric machine cannot be (easily) studied. Consequently, ML-based approaches are typically not considered when there is interest in gaining better understanding of the effects that take place inside electric machines. For instance, discovering that a particular thermal resistance and, thus, the corresponding heat flow, is speed-dependent can hardly be achieved through applying ML-based techniques. This is in contrast to lumped parameter thermal networks (LPTNs) [6]–[8], where basic models lack in flexibility and require all relevant losses as independent inputs. However, a detailed evaluation of the thermal aspects is possible. Consequently, they typically facilitate human-based improvements, e.g., in [9]. The authors consider both, LPTNs as well as ML-based approaches as promising approaches that shall be selected based on the particular application and desired goals to achieve. Here, a detailed analysis of the development of an LPTN-based hybrid thermal modeling approach, starting with the initial selection and modeling refinement, and the subsequent single- and multi-objective optimization of optimal parameter settings will be presented.

II. Motor under test

In this paper, the focus is on a 3-phase, brushless SPM machine in outer rotor topology, which is shown with disassembled rotor bell in Fig. 1. The motor under test has a rated power of $110\,\mathrm{W}$ at $150\,\mathrm{mNm}$ and $7100\,\mathrm{rpm}$. Table I summarizes its most important electrical characteristics. These type of machines are typically used for fan applications in the low-cost segment, for which reason a high utilization for each individual application is desired. A major challenge

Fig. 1: Motor under test with disassembled outer rotor.

TABLE I: Characteristic motor data.

Motor under test: outer rotor SPM	
Rated DC bus voltage	24 V
Rated DC bus current	5.1 A
Number of phases	3
Number of pole pairs	2
Phase connection	Δ
Rated speed	7100 rpm
Rated torque	150 mNm
Terminal resistance (at 20 °C)	0.427 Ω

posed by developing a thermal model for this type of machine is the rotating bell in the ambient air, which causes very complex overall heat flows. Additionally, a large air gap of approximately $4\,\mathrm{mm}$ between the mounting flange and the bell couples the interior with the surrounding air. As a result, an additional air flow depending on the rotor speed and the internal temperatures occurs, and it causes an increased heat exchange. Basically, these phenomena require complex modeling approaches. The authors have consequently chosen a data-based approach to model these characteristics.

III. Evolution of the Thermal Network

The authors presented a five-node LPTN designed for the thermal analysis of the most important motor temperatures of the outer rotor SPM, namely the average temperatures of the rotor (T_r), the air gap (T_air), the stator winding (T_w), the stator lamination (T_s), and the stator fixture including the mounting flange (T_f), in [3]. This network topology, depicted in Fig. 2a, and its initial parameter setting were selected based on expert knowledge and preliminary measurements. First, an individual weighting of the most important machine components combined with the manufacturer's information about their material properties allowed a precise estimation of the heat capacities C_r, C_teeth, C_s, and C_sfix. Then, the uncertain parameters $R_\mathrm{ra,0}$, $R_\mathrm{air,0}$, R_sa, R_ig, $k_\mathrm{ra,s}$, $k_\mathrm{air,s}$, $\Delta R_\mathrm{ra,0}$, $\Delta R_\mathrm{air,0}$, and $\Delta R_\mathrm{sa,0}$ had been optimized through an initial design of experiments (DOE) based sampling, followed by an evolutionary optimization strategy discussed in [3]. Hence, a minimum averaged effective temperature error between modeled and measured temperatures of $e_\mathrm{tot} = 2.28\,^\circ\mathrm{C}$ was achieved. In the following, a stepwise extension of the initial network is proposed, in order to model further temperatures required for a complete thermal monitoring of all critical motor components, but also to further reduce the modeling error for all, both existing and added, temperatures.

A precise monitoring of additional temperatures affecting the motor's lifetime, in particular the temperatures of the inner and outer bearing (T_bi, T_bo), requires a subdivision of the thermal path from stator lamination through stator fixture to ambient into individual parts. Generally, the temperature level and its transient development influence the durability of the bearing grease. Consequently, a load-dependent monitoring of this temperature together with the speed course over its life cycle allows an estimation of the remaining bearing lifetime. For this reason, additional thermal resistors and capacitors are inserted in the heat path, along with two heat sources to consider the bearing losses (P_bi, P_bo), as shown in Fig. 2b and highlighted by dark blue color. A good estimate of the new capacitances C_bi, C_bo, and C_f can be determined from the optimized capacitance C_sfix of the initial network, according to their mass fractions on the entire object, consisting of the stator fixture and flange and their individual material properties. The separation of the thermal resistance R_sa into R_bio, R_sf, and $R_\mathrm{fa}(n)$ is more challenging because of different propagation directions of the heat flow, and the speed dependency of the individual heat transfer mechanisms.

Additionally, detailed investigations based on the initial network indicated the presence of additional cooling paths for the winding system and the stator lamination through the air gap between rotor bell and mounting flange. They can be modeled by two speed-dependent thermal transition resistances $R_\mathrm{cua}(n)$ and $R_\mathrm{sa}(n)$, as depicted in Fig. 2c.

Besides additional thermal resistances and heat capacities, the aforementioned evolution of the initial LPTN also leads to a higher amount of speed dependencies due to natural and forced convection. Since such behavior cannot easily be described by an analytical model, which on the one hand represents reality as accurately as possible, but on the other hand contains as few parameters as possible, the behavior should be calibrated by using an optimization algorithm itself. Thus, three models, shown in Fig. 3, with different characteristics are provided to the optimization algorithm. Note that all models exhibit a steep transition from natural to forced convection starting at zero speed to speeds greater than zero, represented by a delta-distribution. If the thermal resistance additionally decreases linearly with speed, it can be described by

$$R_i(n) = R_{i,0}\left(1 - \frac{|n|}{n_\mathrm{max}}(1 - k_{i,\mathrm{s}})\right) + \Delta R_{i,0}\,\delta(n) \quad , \quad (1)$$

where n is the rotational speed of the rotor bell, $R_{i,0} = R_i(0)$ is the additive thermal resistance value at zero speed, $n_\mathrm{max} = 7500\,\mathrm{rpm}$ is the maximum reachable speed of the rotor bell, $k_{i,\mathrm{s}}$ is the parameter to be optimized, and $\delta(n)$ is the

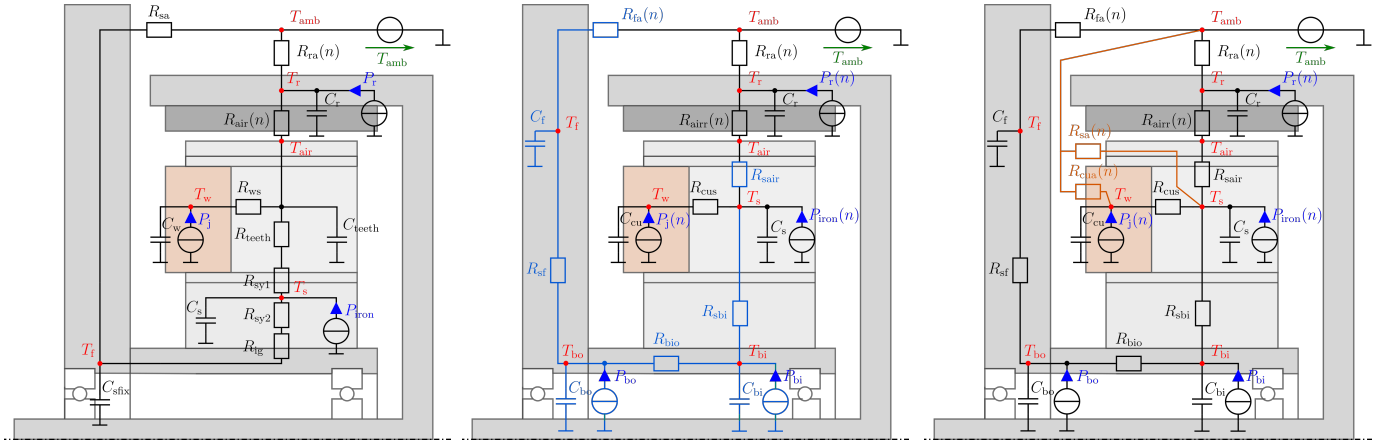

(a) Initial model (b) First evolution (c) Second evolution

Fig. 2: Evolution of the lumped parameter thermal network (LPTN) for modeling the characteristics of outer rotor SPM machines - changes are highlighted by light blue and orange color, respectively.

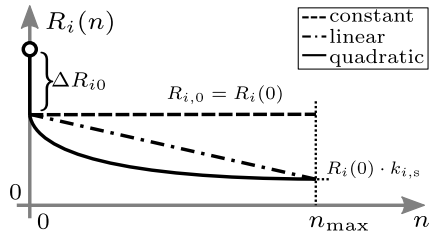

Fig. 3: Three different approaches for modeling the speed-dependent forced convection with a minimum number of parameters.

delta-distribution, already presented in [3]. For many problems, the thermal resistance decreases more than linear with speed. This can be approximated by introducing a quadratic model

$$R_i(n) = R_{i,0}\left(k_{i,s} + \left(\frac{|n|}{n_{max}} - 1\right)^2 (1 - k_{i,s})\right) + \Delta R_{i,0}\,\delta(n) \quad , \tag{2}$$

which requires the same number of parameters as (1). If no relevant change in thermal resistance occurs after the abrupt transition from natural to forced convection due to an increase in speed,

$$R_i(n) = R_{i,0} + \Delta R_{i,0}\,\delta(n) \tag{3}$$

can be used. In order to handle the increased number of parameters, an efficient and improved optimization concept is required. For compensating this rising number of variables to be optimized, serial resistors can be merged, such as R_{sbi} and R_{sair}. Note that besides the introduced extensions will enhance the achievable accuracy of the temperature monitoring, the complexity of the corresponding parameter identification is more challenging and it takes additional effort, as will be discussed in Section V.

IV. Experimental Setup

In order to facilitate a data-based optimization of the parameter presented in the LPTN, a test setup featuring an accurate measurement of the machine's temperatures is essential. Generally, the transient temperature characteristics of individual motor components strongly depend on the dynamic load profile that the machine is exposed to. Thus, a large number of measurements at various load torques and speeds are required to obtain a globally accurate thermal model. Accordingly, an experimental setup shown in Fig. 4 was designed and built up for both the operation of the machine at different operating points by controlling speed and torque with an field-oriented control, and the continuous acquisition of the temperatures defined in the network illustrated in Fig. 2c.
By utilizing the power electronics (a), the stator current excitation is realized to control the speed of the motor under test (b). The desired load torque is applied through a hysteresis brake (c), and it is measured by the torque sensor (d). Furthermore, measuring the total active power consumption at various load points with a power analyzer allows the determination of power losses dissipated within the motor. Based on these measurements, the various power loss sources in the thermal network can be quantified by an individual loss separation method, which already was presented in [3]. All temperatures are measured with thermocouples (type K), and the rotor temperature, which approximately represents the averaged permanent magnet temperature, is acquired by using a thermographic camera shown in Fig. 4. Note that the magnets' temperature cannot be directly measured due to the given motor topology.
Another particular challenge is the identification of temperature profiles to be measured that contain all essential information about the thermal behavior of the PMSM across the entire torque-speed-range and thus allow an optimal identification of the uncertain parameters. Thus, randomly selected speed-

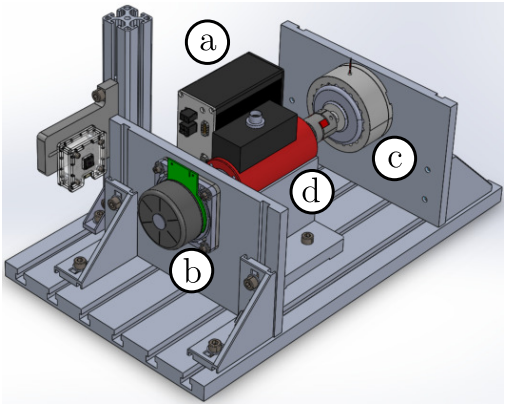

Fig. 4: A CAD model of the test bench for acquiring the thermal characteristics at various operating points.

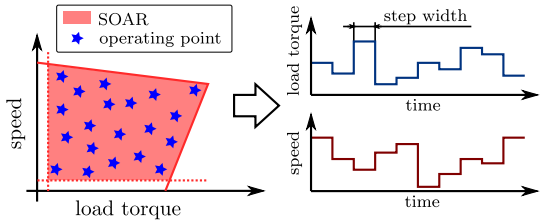

Fig. 5: Random selection of different torque-speed combinations within the SOAR and their transformation into transient load profiles.

torque-combinations within the safe operating area (SOAR) of the SPM, cf. Fig. 5, are converted to transient load profiles to be measured. The specimen is driven at constant speed and load torque for a predefined time interval, defined with a so-called step width. If this parameter is varied as well, both more or less dynamic load profiles can be considered, which results in static and dynamic thermal states in the motor. In this work, the database includes several measurement cycles with 120 h transient temperature curves in total.

Typical resulting transient characteristics of all measured temperatures, the applied speed and torque profile, and the measured total input power are illustrated in Fig. 6. As can be observed, the winding temperatures are the highest, followed by the stator lamination, the inner bearing, and the flange. This is due to the fact that the Joule losses are the dominating loss component. Depending on the rotor's speed, their main cooling takes place either via the stator, the stator fixture and the mounting flange, or via the air gap between bell and mounting flange and the rotor bell itself. More details on the performed measurement series are discussed in [3].

V. Single- and Multi-Objective Based Parameter Optimization

The presented evolution of the LPTN in combination with additional measured data sets by the test bench allow a renewed parameter identification compared to the initially focused approach, that was presented in [3]. Again, the

TABLE II: Optimal parameter set determined by analyzing the single-objective optimization problem.

Parameter at 20 °C	Optimized value
R_{cus}	$2.75\,\mathrm{K\,W^{-1}}$
R_{bi}	$2.49\,\mathrm{K\,W^{-1}}$
R_{bio}	$1.92\,\mathrm{K\,W^{-1}}$
R_{bof}	$0.71\,\mathrm{K\,W^{-1}}$
R_{sair}	$1.85\,\mathrm{K\,W^{-1}}$
$R_{\mathrm{ra,0}}$	$2.57\,\mathrm{K\,W^{-1}}$
$R_{\mathrm{fa,0}}$	$7.19\,\mathrm{K\,W^{-1}}$
$R_{\mathrm{cua,0}}$	$19.47\,\mathrm{K\,W^{-1}}$
$R_{\mathrm{sa,0}}$	$126.10\,\mathrm{K\,W^{-1}}$
$R_{\mathrm{airr,0}}$	$4.53\,\mathrm{K\,W^{-1}}$
$k_{\mathrm{ra,s}}$	0.19
$k_{\mathrm{fa,s}}$	0.52
$k_{\mathrm{cua,s}}$	0.22
$k_{\mathrm{sa,s}}$	0.42
$k_{\mathrm{airr,s}}$	0.60
ΔR_{ra}	$9.1\,\mathrm{K\,W^{-1}}$
ΔR_{fa}	$2.9\,\mathrm{K\,W^{-1}}$
ΔR_{cua}	$31.5\,\mathrm{K\,W^{-1}}$
ΔR_{sa}	$30.1\,\mathrm{K\,W^{-1}}$
ΔR_{airr}	$5.0\,\mathrm{K\,W^{-1}}$

modeling errors for all considered machine's temperatures are combined, and the overall sum is considered for minimization within a single objective optimization scenario. For instance, in case n temperatures are considered, and $T_i(k)$ and $\hat{T}_i(k)$ are the i-th measured and modeled temperature sequence with k representing the sample index, then some formulation like

$$e_{\mathrm{tot}} = \frac{1}{N}\sum_{i=1}^{N}\sqrt{\frac{1}{P}\sum_{k=1}^{P}\left(T_i(k)-\hat{T}_i(k)\right)^2}\,, \tag{4}$$

which gives the root mean squared error (RMSE), is applied. In case of thermal modeling, this quantity can be interpreted as an effective temperature error. By extending and improving the initial approach given in [3], it was possible to reduce the effective temperature error from $e^*_{\mathrm{tot}} = 2.28\,^{\circ}\mathrm{C}$ to $e^*_{\mathrm{tot}} = 0.85\,^{\circ}\mathrm{C}$. The superscript * is used here for indicating a result received through solving a single-objective optimization problem. As can be observed, the results constitute a significant improvement in the modeling accuracy by a factor of 2.7. Comparable improvements would not have been possible with the initially proposed network topology. Table II summarizes the identified parameters based on the single-objective optimization.

While formulations like (4) follow an easier-to-handle optimization problem even in case multiple temperatures are modeled, they neither do provide (too much) insight about the temperature errors of the different components, nor which minimum individual temperature errors could be achieved. Moreover, no potential tradeoff regarding achievable temperature errors for different components can be studied. However, the latter would facilitate a better understanding of how the

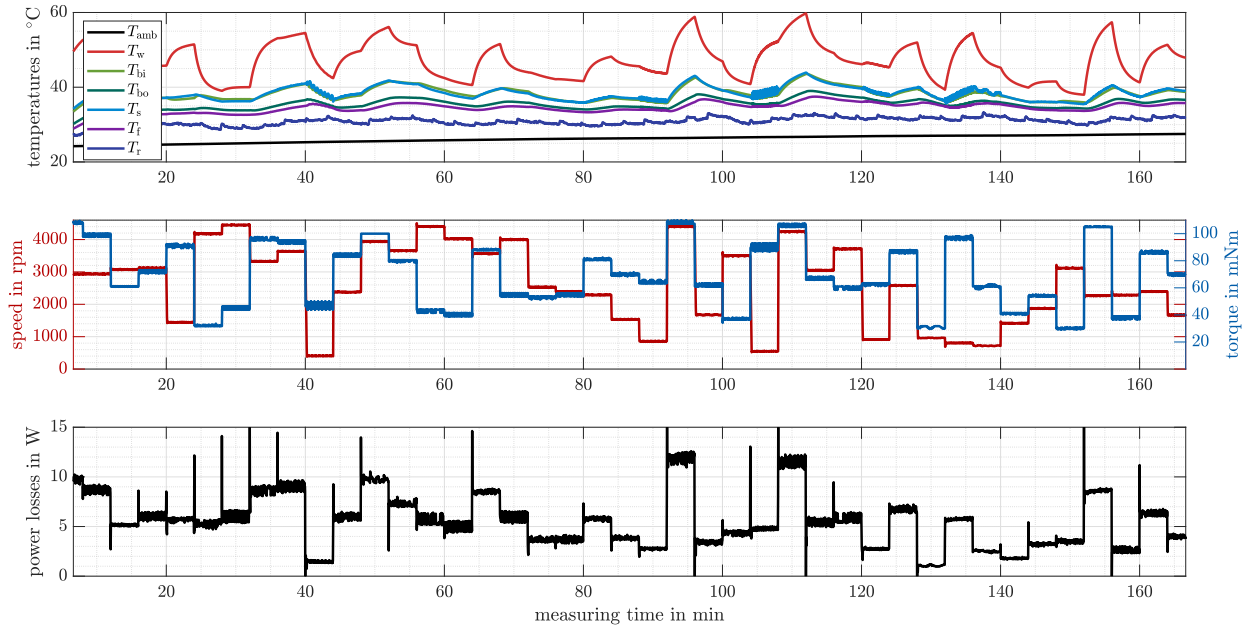

Fig. 6: Characteristic dataset for transient load variations including the motor component's temperatures, the speed and torque signals, and the total power loss of the motor.

model further can be improved. Consequently, the authors also consider a multi-objective formulation for the present problem, with objectives subjected to minimize defined as:

$$\mathbf{e} = \begin{bmatrix} e_\mathrm{w} & e_\mathrm{s} & e_\mathrm{bi} & e_\mathrm{bo} & e_\mathrm{f} & e_\mathrm{r} \end{bmatrix} \tag{5}$$

with

$$e_i = \sqrt{\frac{1}{P}\sum_{k=1}^{P}\left(T_i(k) - \hat{T}_i(k)\right)^2}, \tag{6}$$

and $i \in \{\mathrm{w}, \mathrm{s}, \mathrm{bi}, \mathrm{bo}, \mathrm{f}, \mathrm{r}\}$, where the e_i give the individual six effective temperature errors of the major components of the setup, cf. Fig. 2.

An initial sampling of the design space is performed before the optimization algorithm is applied. The varied parameters include both the nominal values of network elements and several coefficients for modeling the speed-dependencies. Those dependencies were described in detail within Section III.

VI. Results

In order to compare the results of the multi-objective optimization problem with the original results obtained for the single-objective counterpart, all errors were normalized using

$$r_j = \frac{e_j}{e_j^*} \tag{7}$$

with $j \in \{\mathrm{tot}, \mathrm{w}, \mathrm{s}, \mathrm{bi}, \mathrm{bo}, \mathrm{f}, \mathrm{r}\}$. Hence, r_j gives the individual relative errors, and $r_j < 1$ depicts an improvement compared to the single- objective optimization scenario.

The multi-objective optimization problem was analyzed using the software SyMSpace [10], which allows for distributing computationally expensive jobs to a computer cluster. In total, 80,000 parameter combinations were evaluated during the optimization process. The overall results are presented in Fig. 7.

All relative loss values are plotted against each other in matrix form. The plots above the main diagonal represents the results for all investigated combinations, while the maximum values for the plot limits were set to 20 for reasons of visibility. These plots are considered interesting for studying which possible outcomes are possible based on there applied LPTN, cf. Section III. While some measures are strongly correlated, e.g., the total and the inner bearing temperature error r_tot, r_bi in the first row, fourth column, abbreviated as (1,4), or the errors regarding outer bearing and flange temperature estimation r_bo, r_f in (5,6), others feature a far less correlation. In particular, the rotor temperature estimation seems somewhat detached from the temperature estimations for the other components. Along the main diagonal, the same quantity is plotted both on the x- and y-axis. It thus comes as no surprise that the graph depicts an equality relation.

The plots below the main diagonal in Fig. 7 give further insights to this multi-objective optimization problem. The orange-colored markers all give Pareto-optimal results when considering all the temperature errors as objectives. As can be observed, more or less significant improvements can be made compared to the single-objective solution. However, overall the tradeoff regarding these improvements has to be considered, as an improvement in one temperature modeling can cause a degradation for another quantity. By investigating a multi-objective problem, it is possible to study the correlations of the objectives in detail. The gained insights cannot be derived if a single-objective optimization problem is focused.

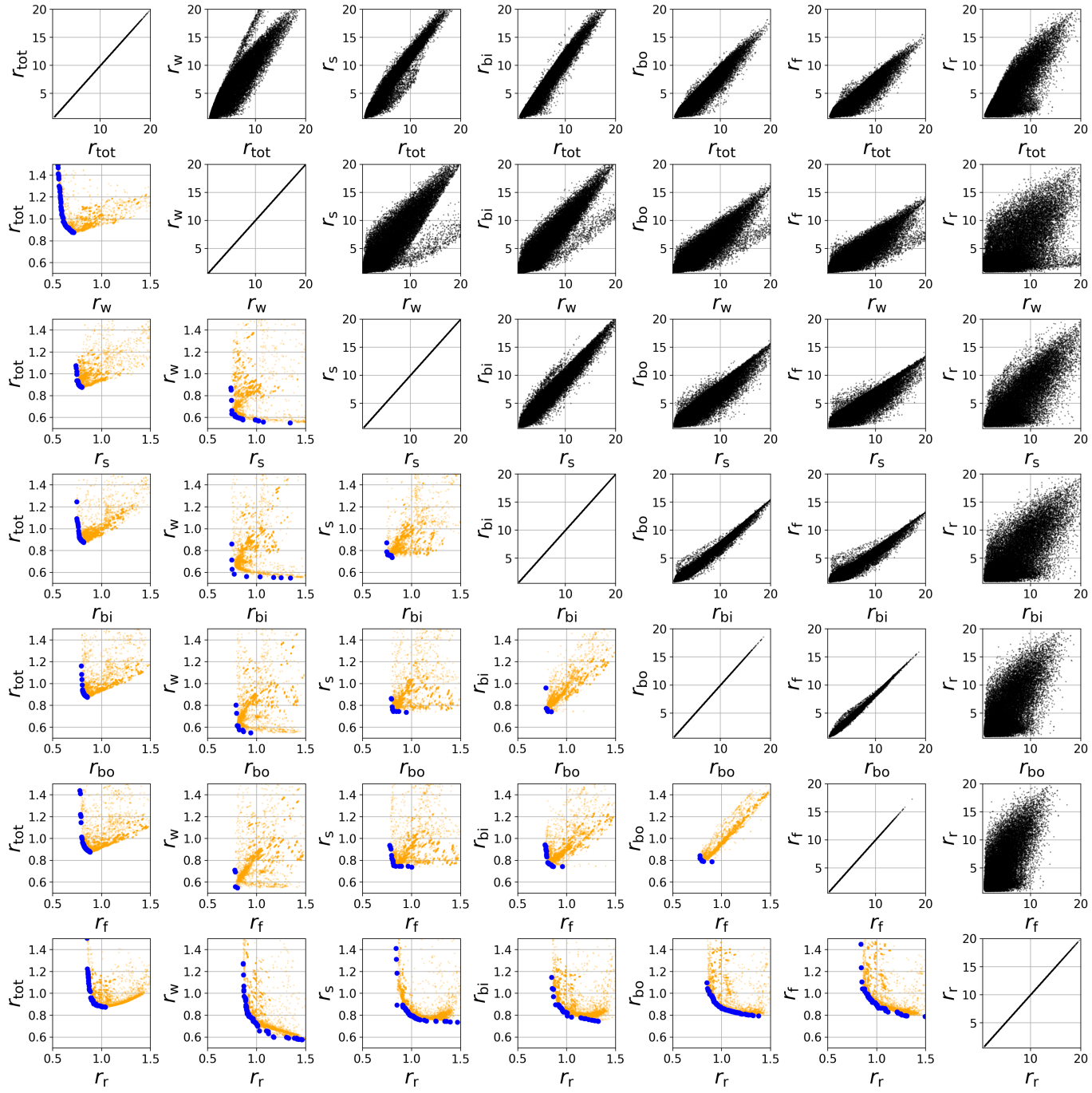

Fig. 7: Results for the multi-objective optimization problem. All errors in temperature modeling r_j are given with reference to the results for the single-optimization problem. The corresponding definition can be found in (7).

Furthermore, the blue-colored markers represent Pareto-optimal results in case only the two quantities of any individual plot would be considered as objectives. For instance, in case the total error r_{tot} and the error in winding temperature estimation r_w would have been considered only, illustrated in (2,1), a potential reduction in (i) the error for the modeled winding temperature ot up to 50% compared to the original value, causing an increase of the total error to 145%, or (ii) both a decrease of the winding-related error to about 75% and the total error to 85% can for instance be accomplished. From the latter it can be concluded that both objectives can simultaneously be significantly improved in case other modeled temperatures are of less interest. This can be interesting in case the focus is on the winding temperature, which considers the hotspot for almost the entire torque speed range for this design, which can also be observed from Fig. 6. In the end, it is the user's choice to decide which objectives are more or less relevant to consider. Obviously, again a weighting can be introduced to finally derive a single parameter setting to be used.

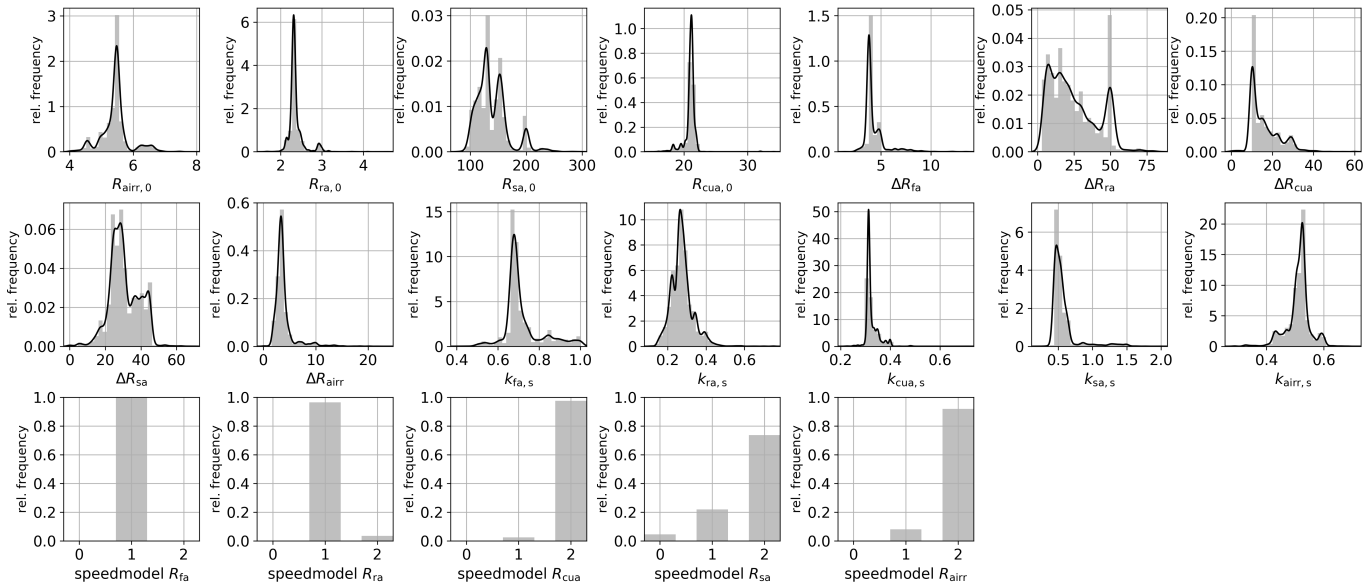

Fig. 8: Relative frequency of particular values set for the design parameters of the multi-objective optimization problem. Only Pareto-optimal designs were considered for this evaluation.

Fig. 8 gives the probability density function (pdf), i.e. a measure for the relative frequency of the parameters' values to appear for the Pareto-optimal designs. Therefore, the Pareto-front for the multi-objective case featuring all seven relative temperature errors was considered. The presented results allow for studying if more or less diverse settings regarding any individual parameter were obtained. For instance, a very distinct small parameter region is observed for $R_{\mathrm{cua},0}$ regarding the Pareto-optimal designs, while for ΔR_{ra} more diverse values were derived.

The plot limits along the x-axis correlate with the minimum and maximum boundary that was set for the individual parameter variation, while no discretization but continuous parameter ranges were specified for the parameters within the first two rows. Based on the pdfs, one can further analyze if the enlargement of some parameter range might follow better results. This most likely is the case if a pdf features a peak value close or at the left or right particular x-axis boundary. In addition, a comparison of the obtained values with parameters solely obtained through applying engineering knowledge facilitates studying the reasonability of the derived values. In case they are considered as unreasonable, the applied modeling must be re-evaluated in more detail and potentially improved.

The bottom row of Fig. 8 contains the parameters that specify the per design selected speed-dependency, as explained in Section III. Hence, only the integer values 0, 1, and 2 are considered for the variation. It is interesting to study the parameters' distribution for the Pareto-optimal results and thus observe if no, a linear, or a quadratic speed dependency follows the best results. Most of the quantities feature a quite distinct preferred setting. Investigating these results in more detail can help understanding the heat flow within outer rotor machines better, which is very complex for this machine type. This particularly holds when considering its speed-dependency. Hence, the results presented here can stimulated future modeling improvements. Future work could be about modeling the speed-dependency as function of multiple components at once, e.g., a linear and a quadratic term, and analyzing if this follows even better results.

VII. Conclusion

This paper was about improvements for measurement-based optimization of thermal models for electric machines by considering a lumped parameter thermal network based approach. As device under test, an outer rotor PM synchronous machine was selected. Modifications of the thermal network for a more accurate temperature modeling were presented, which included the introduction of additional paths for the heat flow, as well as analyzing no, a linear, or a quadratic speed dependency for selected temperature resistors.

The parameters of an existing network were optimized by considering a single-objective problem first. The objective to be minimized was defined based on the temperature modeling errors for the six major parts of the arrangement. In addition, a multi-objective problem was studied. Thereby, the six individual errors for the temperature modeling as well as their particularly defined sum were considered as, in total, seven objectives. The results of the latter optimization problem facilitated studying potential tradeoffs in terms of achievable accuracy with regard to the individual modeling errors. Moreover, investigating the ideal design parameter settings for the Pareto-optimal combinations revealed interesting insights, e.g., about if no, a linear, or a quadratic speed dependency for the individual thermal resistances followed improvements in

modeling accuracy. The results can stimulate further model refinements.

Future work shall include combining multiple temperature-dependent components for modeling the speed dependency of particular resistors at once, as for instance a linear and a quadratic term, and analyzing potential further improvements. Moreover, the temperature dependency of the heat flow paths and the loss development will be studied in more detail.

ACKNOWLEDGMENT

This work has been supported by the COMET-K2 "Center for Symbiotic Mechatronics" of the Linz Center of Mechatronics (LCM) funded by the Austrian federal government and the federal state of Upper Austria. The authors thank ebmpapst St. Georgen GmbH & Co. KG, the manufacturer of the motor under test, who provided the machine for this study.

REFERENCES

[1] S. Nategh, Z. Huang, A. Krings, O. Wallmark, and M. Leksell, "Thermal Modeling of Directly Cooled Electric Machines Using Lumped Parameter and Limited CFD Analysis," *IEEE Transactions on Energy Conversion*, vol. 28, no. 4, pp. 979–990, dec 2013.

[2] P. H. Connor, S. J. Pickering, C. Gerada, C. N. Eastwick, C. Micallef, and C. Tighe, "Computational fluid dynamics modelling of an entire synchronous generator for improved thermal management," *IET Electric Power Appl.*, vol. 7, no. 3, pp. 231–236, mar 2013.

[3] D. Wockinger, G. Bramerdorfer, S. Drexler, S. Vaschetto, A. Cavagnino, A. Tenconi, W. Amrhein, and F. Jeske, "Measurement-Based Optimization of Thermal Networks for Temperature Monitoring of Outer Rotor PM Machines," in *2020 IEEE Energy Conversion Congress and Exposition (ECCE)*. IEEE, oct 2020, pp. 4261–4268. [Online]. Available: https://ieeexplore.ieee.org/document/9236388/

[4] F. Boseniuk and B. Ponick, "Parameterization of transient thermal models for permanent magnet synchronous machines exclusively based on measurements," *Intern. Symp. on Power Electr., Electrical Drives, Automation and Motion (SPEEDAM)*, pp. 295–301, 2014.

[5] W. Kirchgassner, O. Wallscheid, and J. Bocker, "Estimating Electric Motor Temperatures with Deep Residual Machine Learning," *IEEE Transactions on Power Electronics*, pp. 1–1, 2021. [Online]. Available: https://ieeexplore.ieee.org/document/9296842/

[6] P. Giangrande, V. Madonna, S. Nuzzo, C. Spagnolo, C. Gerada, and M. Galea, "Reduced order lumped parameter thermal netw. for dual three-phase permanent magnet mach." *IEEE Worksh. on Electr. Mach. Design, Contr. and Diagn., WEMDCD 2019*, pp. 71–76, 2019.

[7] A. Boglietti, A. Cavagnino, D. Staton, M. Shanel, M. Mueller, and C. Mejuto, "Evolution and modern approaches for thermal analysis of electrical machines," in *IEEE Transactions on Industrial Electronics*, 2009.

[8] A. Adouni and A. J. M. Cardoso, "Thermal Analysis of Synchronous Reluctance Machines – A Review," *Electric Power Components and Systems*, vol. 47, no. 6-7, pp. 471–485, apr 2019.

[9] B. Assaad, K. El Kadri Benkara, G. Friedrich, S. Vivier, and A. Michon, "Reducing the complexity of thermal models for electric machines via sensitivity analyses," *2017 IEEE Energy Conv. Congr. and Exposition (ECCE)*, vol. 2017-Janua, pp. 4658–4665, 2017.

[10] S. Silber, W. Koppelstätter, G. Weidenholzer, G. Segon, and G. Bramerdorfer, "Reducing development time of electric machines with symspace," in *2018 8th International Electric Drives Production Conference (EDPC)*, Dec 2018, pp. 1–5.